1980ApJ...237...26H

THE ASTROPHYSICAL JOURNAL, 237:26–37, 1980 April 1
© 1980. The American Astronomical Society. All rights reserved. Printed in U.S.A.

OBSERVATIONS OF A COMPACT H II REGION AND WATER VAPOR MASER SOURCES IN THE VICINITY OF THE HERBIG-HARO OBJECTS 7–11

A. D. HASCHICK,[1] J. M. MORAN, L. F. RODRIGUEZ[2]
Harvard-Smithsonian Center for Astrophysics
AND
B. F. BURKE, P. GREENFIELD, AND J. A. GARCIA-BARRETO
Research Laboratory of Electronics, Massachusetts Institute of Technology
Received 1979 August 13; accepted 1979 October 19

ABSTRACT

The H_2O maser source near the Herbig-Haro objects H-H 7–11, which has velocity components between -10 and -30 km s^{-1}, was monitored at approximately monthly intervals over a period of three years. Two additional sites of maser emission were discovered at velocities close to the ambient cloud velocity of 8.3 km s^{-1} but separated from the original maser source by 0.5 and 2.5, respectively. The time variations both in velocity and intensity of all three sources are characterized by periods of rapid activity lasting about 1 year, followed by a period of months to years in which the maser is unobservable within our sensitivity limits. Two of the maser sources abruptly turned on within 10 days of each other after an 18 month period of quiescence. These masers may have a common maser pump. We discovered a compact H II region coincident in angle with one of the masers. A VLBI measurement showed that the maser had an unusually small apparent size of about 3×10^{12} cm. The observations are discussed with reference to theories of H-H objects.

Subject headings: interstellar: molecules — masers — nebulae: general — stars: pre–main-sequence

I. INTRODUCTION

The boundary of the dark cloud complex L1450, which is southwest of the reflection nebula NGC 1333 contains young stellar objects covering a wide range in age. These include Hα-emission objects (Herbig and Rao, 1972), Herbig-Haro (H-H) objects (Herbig 1974; Strom, Grasdalen, and Strom 1974), and at least one T Tauri star. Several 2.2 μm infrared objects have also been discovered in this complex by Strom, Vrba, and Strom (1976). The distance to these objects was estimated to be 500 pc by Strom, Grasdalen, and Strom (1974). NGC 1333 has been included in a number of radio surveys. Lada *et al.* (1974) mapped the millimeter-wave emission lines from HCN, H_2CO, and CS, and derived a mean molecular cloud velocity of 8.3 km s^{-1}. Loren (1976), in a CO survey of the region, observed two clouds with velocities of 6.3 and 8.3 km s^{-1}, respectively. Self-absorption was present at 8.3 km s^{-1} in the vicinity of the Herbig-Haro objects, H-H 7–11. Loren proposed a two cloud collision model to explain the young stellar objects.

A water vapor maser was detected close to both H-H 11 and a 2.2 μm infrared source (Lo, Burke, and Haschick 1975; Dickinson, Kajoian, and Strom 1974). The H_2O spectrum was blueshifted by 20–50 km s^{-1} with respect to the molecular cloud velocity and exhibited rapid variations in velocity and amplitude over periods of days to weeks (Lo *et al.* 1976; White and Little 1975). The H-H objects also exhibit large blueshifts in their velocities of 30–150 km s^{-1} as well as optical variability over the period of months to years (Strom, Grasdalen, and Strom 1974). The appearance in 1975 July of a maser feature near the velocity of the molecular cloud suggests that the H_2O maser may provide a way of probing unusual kinematic structure near the H-H objects.

We report on a 3 year monitoring program of the H_2O maser emission in the vicinity of the H-H objects 7–11. Two new H_2O maser sites were detected. The results of a very long baseline interferometric (VLBI) study of one of the masers and sensitive continuum observations of the area containing the H_2O sources are reported. An unsuccessful search for OH masers from this region was made. These results are discussed with reference to existing theories of the formation of H-H objects such as the "interstellar bullet" theory of Norman and Silk (1979) and Rodriguez *et al.* (1979).

II. OBSERVATIONS

a) H_2O *Observations*

The time monitoring observations of the H_2O maser source near H-H 7–11 were conducted at the Haystack Observatory[3] 36.6 m antenna from 1974 July

[1] Also associated with the Research Laboratory of Electronics, Massachusetts Institute of Technology.

[2] Also associated with the Instituto de Astronomía, Universidad Nacional Autónoma de Mexico.

[3] Haystack Observatory is operated by the Northeast Radio Observatory Corporation with support from the National Science Foundation.

© American Astronomical Society • Provided by the NASA Astrophysics Data System

1980ApJ...237...26H

to 1978 April. The antenna beamwidth was 1'.5 at the H_2O rest frequencx of 22.23508 GHz. The sensitivity, which varies with atmospheric conditions and elevation angle, was measured during most of our observations using the sources 3C84 and DR21 for calibration. Values of the flux densities for 3C84 were obtained from Balonek (1979). For typical conditions at 50° elevation the sensitivity is ~ 13.5 Jy K^{-1}, and at 20° elevation, ~ 17 Jy K^{-1}. On some occasions an atmospheric model was used to calibrate the data. The maser amplifier receiver had a system temperature in the range of 100–200 K. Prior to 1976 December the 100 channel autocorrelator was used providing a spectral resolution of 2.2 km s^{-1} for a bandwidth of 6.67 MHz. Subsequently, the 1024 channel autocorrelator was employed having a resolution of 0.22 km s^{-1}. Spectra of H-H 7–11 were taken using a 5 minute on-source and 5 minute off-source observation, providing spectra having a typical peak-to-peak noise of 0.3 K. The antenna pointing was checked on each occasion using right ascension and declination scans of 3C84 which is offset from H-H 7–11 by only 10°. The H_2O maser source position was determined by interpolating a grid of observations separated by a half beamwidth or by using right ascension and declination scans. During most observing runs after 1976 December, the region surrounding H-H 7–11 was searched for further H_2O sources using a 3 × 5 full-beamwidth grid centered on the position of H-H 11.

A summary of the time monitoring observations is given in Table 1, which includes the velocity range searched and the estimated flux density and velocity of the detected spectral features. Data for measurements prior to 1976 July were reported by Lo *et al.* (1976). Two further H_2O maser sources, called source B and source C, were detected during the survey and were separated from the original H_2O maser, source A, by $\sim 0'.5$ and $2'.5$, respectively. Both had velocities close to the molecular cloud velocity. The positions of the H_2O masers, H-H objects, and IR sources are shown on a map of the NH_3 emission in Figure 1.

The spectra for times in which a maser was detected are shown in Figures 2 and 3. Both sources A and B lie within the beam of the Haystack antenna and are both shown in these figures. The maser features in source A lie in the velocity range of −35 to −7 km s^{-1}, whereas those in source B occur exclusively at velocities in the range of 2–9 km s^{-1}. The spectra for source C are shown in Figure 4 for two epochs. For all three sources the features are always blueshifted with respect to the molecular cloud.

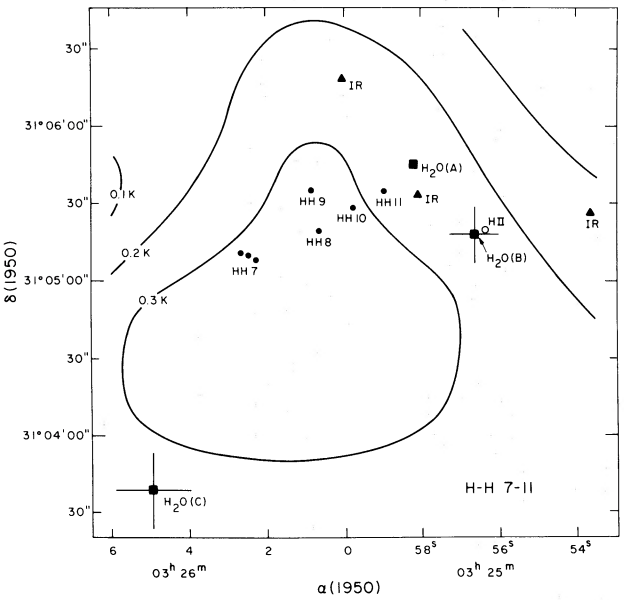

FIG. 1.—Map of the H-H 7–11 region indicating the positions of the H_2O masers (*squares*), the IR sources (*triangles*), the 6 cm continuum source (*open circles*), and the H-H objects (*filled circles*). The accuracy of the positions of the IR sources is ±7″. The contours are of the NH_3 brightness distribution measured on the Haystack Antenna by Ho (1977).

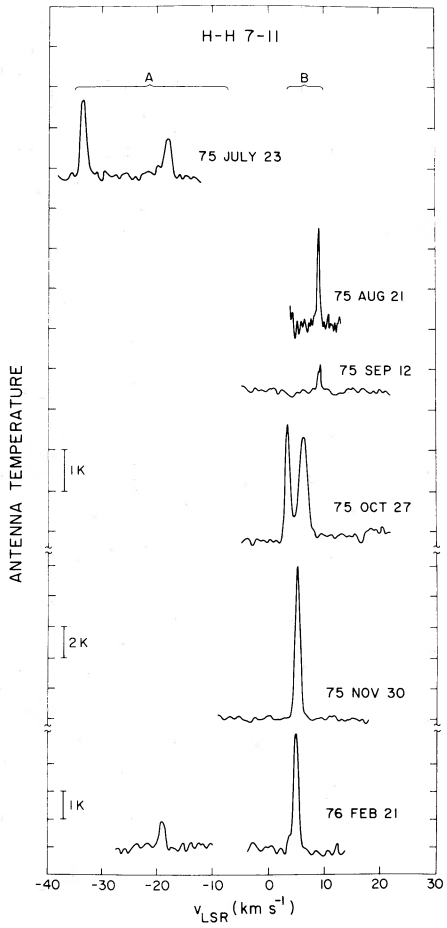

FIG. 2.—Spectra of the H-H 7–11 H_2O maser sources A and B taken at the Haystack Observatory (see map in Fig. 1). The velocity axis refers to the local standard of rest and is based on a rest frequency of 22235.080 MHz. The A source has negative velocities (−33 to −7 km s^{-1}) and the B source has positive velocities (2–9 km s^{-1}). The spectra have not been corrected for gain variations in the antenna nor atmospheric absorption. The corrected flux densities for the features are given in Table 1 along with the velocity resolution.

© American Astronomical Society • Provided by the NASA Astrophysics Data System

1980ApJ...237...26H

TABLE 1

SUMMARY OF SPECTRAL FEATURES IN H_2O MASERS[a]

DATE	VELOCITY RANGE SEARCHED (km s^{-1})	VELOCITY RESOLUTION (km s^{-1})	FLUX LIMIT (5 σ) Jy	A		B		C	
				V_{LSR} (km s^{-1})	S (Jy)	V_{LSR} (km s^{-1})	S (Jy)	V_{LSR} (km s^{-1})	S (Jy)
75 July 5	−38 − 12	0.7	4	−33.6	11	...	...	...	...
				−19.2	98	...	...	...	...
75 July 23	−40 − 14	0.7	4	−33.8	21	...	...	...	...
				−18.6	10	...	...	...	...
75 Aug 21	−195 + 12	2.3	2	...	...	8.7	39	...	...
75 Sep 12	−66 + 24	2.3	5	...	...	8.7	11	...	...
75 Oct 27	−195 + 170	2.3	5	...	...	5.9	45	...	...
						2.9	55	...	...
75 Nov 4	−10 + 16	0.7	6	...	...	3.6	86	...	...
						4.8	50	...	...
75 Nov 30	−170 + 170	2.3	4	...	–	4.8	230	...	...
76 Feb 21	−195 + 194	2.3	3	−19.1	13	4.9	61	...	...
76 Apr 9	−37 + 53	2.3	3	...	–	...	–	...	...
76 May 23	−170 + 170	2.3	3	...	–	...	–	...	...
76 Jun 11	−170 + 170	2.3	5	...	–	...	–	...	...
76 Jul 9	−170 + 170	2.3	4	...	–	...	–	...	...
76 Nov 16	−90 + 90	0.9	4	...	–	...	–	...	...
76 Dec 7	−110 + 70	0.9	3	...	–	...	–	7.3	8
77 Jan 9	−110 + 70	0.9	3	...	–	...	–	–	–
77 Feb 8	−110 + 70	0.9	3	...	–	...	–	–	–
77 Mar 16	−110 + 70	0.9	3	...	–	...	–	–	–
77 Apr 15	−110 + 70	0.9	3	...	–	...	–	5.7	8
								3.4	5
77 Apr 16	−37 + 53	0.2	4	...	...	...	...	5.6	6
								3.4	5
77 May 8	−110 + 70	0.9	5	...	–	...	–	...	–
77 Jun 19	−110 + 70	0.9	5	...	–	...	–	...	–
77 Jul 18	−110 + 70	0.9	6	...	–	...	–	...	–
77 Aug 19	−110 + 70	0.9	5	...	–	...	–	...	–
77 Sep 1	−110 + 70	0.9	5	−9.9	43	7.5	13	...	–
77 Oct 10	−45 + 45	0.2	7	−11.5	44	...	–	...	–
77 Nov 8	−45 + 45	0.2	5	−7.4	140	...	–	...	–
				−15.6	21	...	...	...	...
				−17.7	8	...	...	...	...
77 Nov 9	−55 + 35	0.2	6	−7.4	97	...	–	...	...
				−15.4	11	...	...	...	...
77 Nov 12	−23 + 4	0.1	6	−7.3	92	...	–	...	...
				−15.7	11	...	...	...	...
				−17.3	6	...	...	...	...
77 Dec 7	−55 + 35	0.2	5	−14.2	9	...	–	...	–
				−12.7	10	...	...	...	...
77 Dec 13	−45 + 45	0.2	3	−9.4	5	...	–	...	–
				−10.2	18	...	...	...	...
				−12.8	48	...	...	...	...
				−23.1	3	...	...	...	...
78 Jan 12	−45 + 45	0.3	3	−9.4	72	...	–	...	–
				−10.5	178	...	...	...	...
				−12.5	18	...	...	...	...
78 Feb 17	−45 + 45	0.3	4	−8.9	310	...	–	2.3	9
				−9.8	120	...	...	...	...
				−12.1	20	...	...	...	...
78 Mar 5	−100 + 80	0.9	3	−9.3	200	...	–	2.4	9
				−12.8	5	...	...	...	...
78 Apr 19	−55 + 35	0.2	8	−9.4	19	...	–	...	–
				−10.5	260	...	...	...	...

[a] Flux densities have been corrected for gain variation in the antenna and for atmospheric absorption. The rms error in amplitude calibration is about 15% and the error in velocity is about 0.2 km s^{-1}. A dash denotes no detection, and no entry denotes no observation.

b) Interferometric Observations of the H_2O Maser Source A

VLBI observations of the H_2O maser source A were conducted during a 3 hour period on 1977 November 12. The elements of the interferometer were the 37 m antenna of the Haystack Observatory, the 100 m antenna of the Max Planck Institute for Radio Astronomy (MPI) in Effelsberg, Germany, the 20 m antenna of the Onsala Space Observatory, in Onsala, Sweden, and the 22 m antenna of the Crimean Astrophysical Observatory in Semeis, Crimea, USSR. Data were recorded on the Mark II terminals and processed at the National Radio Astronomy Observa-

© American Astronomical Society • Provided by the NASA Astrophysics Data System

1980ApJ...237...26H

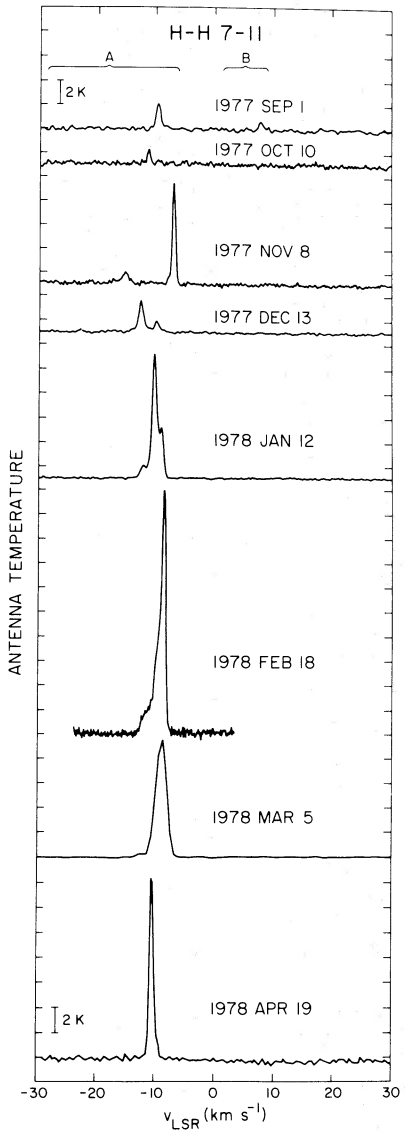

FIG. 3.—More spectra of the H-H 7–11 H_2O maser sources A and B taken at the Haystack Observatory.

tory (NRAO)[4] in Charlottesville, Virginia. The observations consisted of three 15 minute runs on each of the sources: H-H 7–11, W3(OH), and NRAO 150. The spectrum of the maser source A on the date of the observations is shown in Figure 5. It consisted of a narrow feature of 0.5 km s^{-1} width at -7.3 km s^{-1} with a flux density of about 100 Jy and two weaker features near -15.7 and -17.3 km s^{-1}.

The distribution of data as a function of projected baseline (*uv* plane) coordinates is shown in Figure 6 for H-H 7–11. The observations are labeled by numbers, and the corresponding baselines are given in the figure captions. Because of the proximity of the MPI and Onsala telescopes there is some redundancy in the data, since there is no evidence that there is a

[4] NRAO is operated by Associated Universities Inc., under contract with the National Science Foundation.

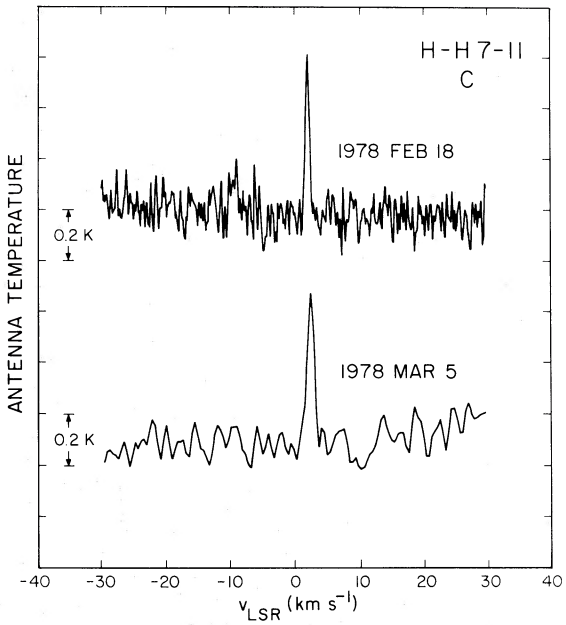

FIG. 4.—Spectra for two epochs of the H-H 7–11 H_2O maser source C taken at the Haystack Observatory.

source structure on the scale of larger than 0".1, as will be evident from the following discussion. In particular the visibilities on the data pairs, 11–13, 14–12, and 7–6 should be about the same (see Fig. 6). In fact, the visibilities were lower for data on the Onsala-Haystack and Onsala-Crimea as compared to the data on the MPI-Haystack and MPI-Crimea baselines by a factor of 1.3. We therefore corrected all data on Onsala baselines by the factor of 1.3. No other corrections were made.

The visibility of the -7.3 km s^{-1} feature as a function of projected baseline length is shown in Figure 7. The data points are numbered for comparison with Figure 6. The visibilities show a general monotonic decrease with increasing baseline. The maximum visibility on the shortest baseline is about 0.9. This could indicate the presence of an extended component of diameter greater than 5 milliarcsec with 10% of the flux density. The more likely explanation is that there is a general 10% loss in coherence due to local oscillator noise. We favor the latter explanation.

The visibility data have several possible interpretations. The model of a single Gaussian disk component does not fit the data very well because of the rapid drop in visibility between 1 and $2 \times 10^8\lambda$, followed by the much slower decline between 4 and $6 \times 10^8\lambda$. For comparison, the visibilities for Gaussian disk models with diameters (full width at half maximum) of 0.3 and 0.4 milliarcsec are shown on Figure 7. Hence, the data definitely show that the visibility decreases more slowly than a single Gaussian component model. A better fit to the data is obtained with a two component Gaussian model which has 60% of the flux density in a component of 0.5 milliarcsec and 40% in a component of 0.2 milliarcsec. At a distance of 500 pc these angular sizes correspond to linear diameters of 3.8 and 2.2×10^{12} cm, respectively. Since the

© American Astronomical Society • Provided by the NASA Astrophysics Data System

1980ApJ...237...26H

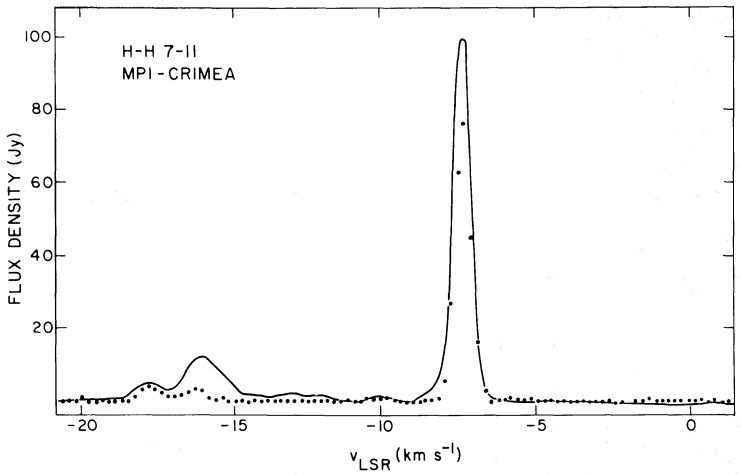

FIG. 5.—Total power spectrum (*solid line*) of the maser in H-H 7–11 (A) taken from VLBI recording made at MPI on 1977 November 12, and a cross power spectrum (*dotted*), corresponding to data point 8 on Figs. 6 and 7, on the MPI-Crimea baseline. The resolution, with uniform weighting, is 0.34 km s^{-1}.

long baselines are nearly east-west in orientation, these sizes correspond to the dimension in the right ascension direction. There is a suggestion that the visibilities increase with increasing north-south baselines (see 11–12, and 13–14–15 data sequences in Figs. 6 and 7). This may indicate that the size of the source is even smaller in the north-south direction. Another possible model is one with two equal components having angular diameters of 0.2 milliarcsec, separated by 0.6 milliarcsec. In this case data points 10–17 (Fig. 7) occur on the second maximum, and nulls in the visibility function would be expected near 2×10^8 and 6×10^8 λ in projected baseline. For all of these models the peak brightness temperature is about 2×10^{13} K. Although this maser is not the brightest, it is one of the smallest ever measured. The image of the maser is probably not affected by interstellar seeing.

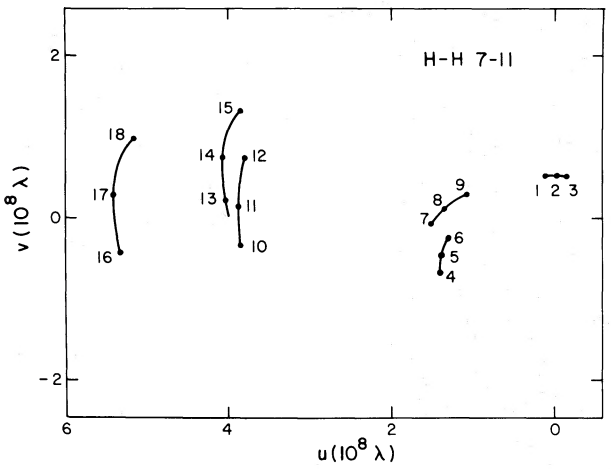

FIG. 6.—Projected baseline loci for the six interferometer pairs, with numbered points marking the places where data were taken. The baselines were: MPI-Onsala (1, 2, 3); Onsala-Crimea (4, 5, 6); MPI-Crimea (7, 8, 9); Haystack-MPI (10, 11, 12), Haystack-Onsala (13, 14, 15); Haystack-Crimea (16, 17, 18).

The estimate of interstellar scattering from free electrons at a distance of 500 pc in the galactic plane is about 0.05 milliarcsec (Duffett-Smith and Readhead 1976), which is about 40 times smaller than the smallest scale size we measured.

The size we observed in our VLBI experiment is very close to the turbulent size scale estimated by Lo *et al.* (1976) who used indirect arguments based on the time scale for variations. This suggests that the maser variability is due to mass motions in the masing gas.

The feature at -7.3 km s^{-1} seems to be quite isolated with little evidence of blending of components at different velocities. In Figure 8 a cross power spectrum from the Haystack-MPI baseline (data point 11 on Figs. 6 and 7) and the total power spectrum are plotted with the amplitude scales adjusted so that a detailed comparison of the profiles can be made. The visibility of the -7.3 km s^{-1} feature is actually 0.25. The profiles are almost exactly the same except in the low velocity wing. There is probably a weak component near -8 km s^{-1} which is resolved on this baseline. Hence, except for this small blending, this feature appears to be a single isolated maser component localized to a region of diameter 0.6 milliarcsec or less. For the model of an unsaturated spherical maser the visibility would be slightly lower in the wings of the line as compared to the center, since the apparent size of the maser would be proportional to the reciprocal of the square root of the gain coefficient. Since the gain coefficient is probably about 25 at the line center, and 24 at the e^{-1} point, the change in visibility would be only about 3%. This effect is very small, and difficult for us to measure. It does not appear to be present.

The structure of the features near -15.7 and -17.3 km s^{-1} are not well determined, since they were too weak to be detectable on the longer baselines. The feature at -17.3 km s^{-1} has a diameter of about 0.3 milliarcsec. The one at -15.7 km s^{-1} is probably blended and may be somewhat larger. We compared the fringe rates among the three features and found no measurable differences on any baseline. Therefore

© American Astronomical Society • Provided by the NASA Astrophysics Data System

1980ApJ...237...26H

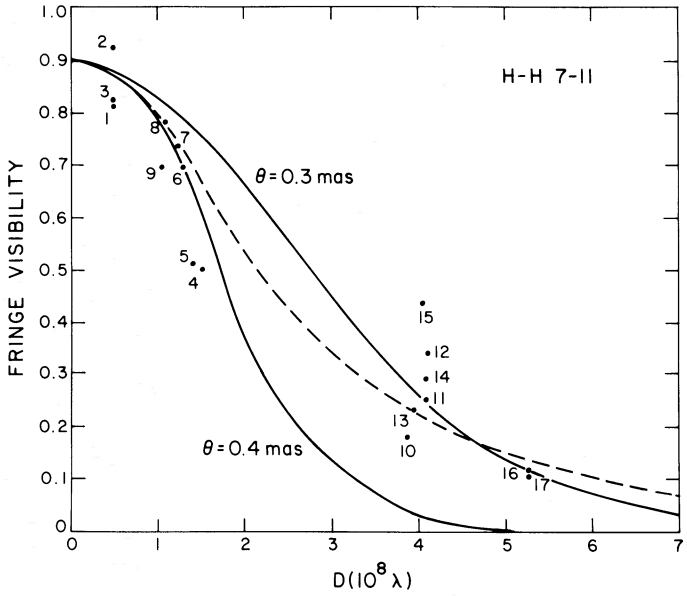

FIG. 7.—Fringe visibility of the -7.3 km s^{-1} feature versus projected baseline. The solid lines are the visibilities for Gaussian disk models having angular diameters (FWHM) of 0.3 and 0.4 milliarcsec. The dashed curve corresponds to a composite Gaussian model with sizes of 0.2 milliarcsec (40% of flux) and 0.5 milliarcsec (60% of the flux). The data points are numbered for comparison with Fig. 6.

the -17.3 and -15.7 km s^{-1} features are coincident with the one at -7.3 km s^{-1} to within ± 5 milliarcsec. The maser region is therefore extremely compact, smaller than 7×10^{13} cm in diameter. The coincidence of these features with velocities differing by 10 km s^{-1} is puzzling. Genzel *et al.* (1979) have shown that neither the Stark effect, the Zeeman effect, nor various plasma effects can produce frequency differences of this magnitude, so they must be kinematic. The scale size of 7×10^{13} cm is too small for the maser components to be situated in a circumstellar shell. The masing cloud must therefore be an isolated fragment with a mass of about $10^{-5}\ M_\odot$ and is currently confined to a diameter of 7×10^{13} cm, but is dispersing at 10 km s^{-1}. The time scale for dispersal of the maser cloud is therefore about a year, which is only three times the lifetime of the masing phenomenon for these particular features (see Fig. 2). Alternatively, if the mass flow from the exciting star creates long radial filaments (Norman and Silk 1979) then only those masers aligned along the line of sight to the star would be observed. In this case the projected separation would be much smaller than the actual distance between the maser features. This model may be unrealistic, since radial velocity gradients would limit the maser gain.

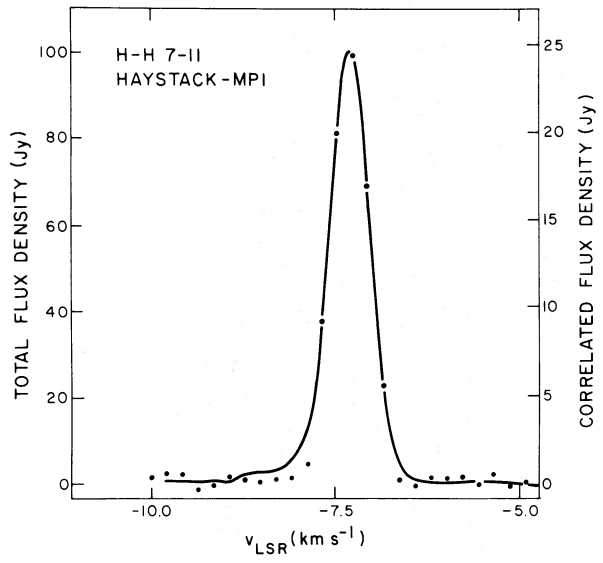

FIG. 8.—Part of the total power spectrum (*solid line*) and the cross power spectrum (*dotted line*) from observation 11 (Haystack-MPI). The amplitude scales have been adjusted to make the spectra overlap. No cross power was detected from the features at -15.7 and -17.3 km s^{-1}.

The absolute fringe rates of the -7.3 km s^{-1} feature were used to determine the position of the maser. NRAO 150 and the H_2O maser in W3(OH) were used as calibrator sources. The position of the maser in H-H 7–11 was estimated on each baseline separately and the results averaged. The averaged position is $\alpha(1950) = 03^h25^m58^s.2 \pm 0^s.1$ and $\delta(1950) = 31°05'44'' \pm 1''$. This is a refinement of the position for source A.

c) *Continuum Observations*

Observations of the continuum emission from the H-H 7–11 region were made in 1978 June using 10 elements of the Very Large Array (VLA), under construction by the NRAO near Socorro, New Mexico. Details of these observations are discussed elsewhere (Rodriguez *et al.* 1979), and only pertinent points will be mentioned here. The resolution of the instrument at the observing frequency of 4.9 GHz was 1″, and the coherent field of view was 5′ for a bandwidth of 50 MHz. The calibration source 0333+321, located

© American Astronomical Society • Provided by the NASA Astrophysics Data System

1980ApJ...237...26H

TABLE 2

POSITIONS FOR THE H_2O MASER, 6 CENTIMETER CONTINUUM, AND 2 MICRON IR SOURCES IN THE H-H 7–11 REGION

Source	R.A. (1950)	Decl. (1950)	NH_3 Velocity[a] (km s^{-1})	H-H Velocity[b] (km s^{-1})	Position Reference
H_2O(A).....	03^{h}25^{m}58^{s}2 ± 0.1	31°05′44″ ± 1	8.0	...	VLBI[c]
H_2O(B).....	03 25 56.6 ± 0.7	31 05 19 ± 10	7.8	...	HSTK
H_2O(C).....	03 26 05.0 ± 1	31 03 40 ± 15	7.6	...	HSTK
Continuum....	03 25 56.38 ± 0.04	31 05 20.3 ± 0.5	7.8	...	VLA
IR(13).....	03 25 58.1 ± 0.5	31 05 33 ± 7	8.0	...	KPNO[d]
IR(14).....	03 26 0.1 ± 0.5	31 06 18 ± 7	8.2	...	KPNO
IR(16).....	03 25 53.7 ± 0.5	31 05 26 ± 7	8.0	...	KPNO
H-H 7.....	03 26 02.5	31 05 13	7.8	−51	LICK[e]
H-H 8.....	03 26 00.7	31 05 19	7.9	−37	LICK
H-H 9.....	03 26 00.9	31 05 35	8.0	...	LICK
H-H 10.....	03 25 59.8	31 05 28	7.9	−22	LICK
H-H 11.....	03 25 59.0	31 05 35	8.0	−139	LICK

[a] Ho and Barrett 1979. Velocity with respect to local standard of rest.
[b] Strom, Grasdalen, and Strom 1974.
[c] This paper.
[d] Strom, Vrba, and Strom 1976.
[e] Herbig 1974.

~2° from H-H 7–11, was observed for 5 minutes, followed by a 10 minute observation on source. Approximately 20 observations were made at different hour angles, and the final map was constructed using 400 iterations of the clean algorithm described by Högbom (1974).

A compact radio source of 1.5 mJy was detected coincident with the H_2O maser source B. No other sources stronger than 0.5 mJy were detected in the field of view. This source was unresolved and smaller than 0″.4. The expected size based on the model of Panagia and Felli (1975), in which the electron density decreases as r^{-2}, is about 0″.1. Its position together with the positions of the three 2.2 μm IR sources, stronger than 10th K magnitude and the three H_2O maser positions are listed in Table 2 and plotted in Figure 1. The cleaned VLA map of this H II region is shown in Figure 9. Some parameters of the H II region are listed in Table 3. The electron density, the mass of the H II region, the emission measure and ionizing photon flux, were calculated using formulas given by Schraml and Mezger (1969), assuming a uniform, spherical, optically thin H II region. The zero-age main sequence (ZAMS) spectral type and luminosity of the star required to maintain the observed ionization were determined from tabulations of Panagia (1973). The spectral type is at least as early as B3, with a luminosity of $10^3\ L_\odot$. This estimate is a lower limit on the luminosity because: (1) the star may still be approaching the main sequence, and its surface temperature and ionizing flux are smaller than what they will be on arrival at the main sequence; (2) the H II region may be optically thick which would result in an underestimate of the electron density and thus reduce the estimate of the ionizing photon flux; and (3) dust may be absorbing the ionizing photons resulting in an underestimate of the stellar ionizing flux.

d) OH

A search for OH maser emission in the vicinity of the H-H objects 7–11 was conducted on the NRAO 43 m telescope in 1979 April. A dual channel cooled parametric amplifier receiver was employed with the 413 channel Mark II autocorrelation spectrometer. The system temperature was ~60 K, and the sensitivity of the antenna at 1667 MHz was ~3.6 Jy K^{-1}. The antenna half-power beamwidth was ~18′ at this frequency. Total power observations were made using crossed linearly polarized feeds. A bandwidth of 1250 kHz was used giving a velocity coverage of 225 km s^{-1} and a resolution of 1.4 km s^{-1} with uniform weighting. The total integration time for each of the four ground state transitions was about 200 minutes. The spectra are shown in Figure 10.

We detected OH emission at a velocity of 8 km s^{-1} at the 1667, 1665, and 1720 MHz transitions. The line ratios $T(1667)/T(1665)$, $T(1667)/T(1720)$, and $T(1667)/T(1612)$ are expected to be 1.8, 9, and 9 under the assumption of LTE conditions for thermally excited gas which is optically thin. The ratios we observed are ~2, ~2.5, and >4. These are slightly anomalous but consistent with the values observed for other dark clouds by Turner (1973), where

TABLE 3

PROPERTIES OF THE H II REGION NEAR H-H 7–11[a]

Flux Density at 4.9 GHz (mJy).....	1.5 ± 0.2
Measured Size (arcsec).....	≤0.4
Electron Density (cm^{-3}).....	≥5 × 10^4
Mass of H II Region ($M_\odot$).....	≤2 × 10^{-6}
Emission Measure (cm^{-6} pc).....	≥4 × 10^6
Photon Flux (s^{-1}).....	3 × 10^{43}
Optical Depth at 4.9 GHz.....	≥0.05

[a] Electron temperature assumed to be 10^4 K, D = 500 pc.

© American Astronomical Society • Provided by the NASA Astrophysics Data System

1980ApJ...237...26H

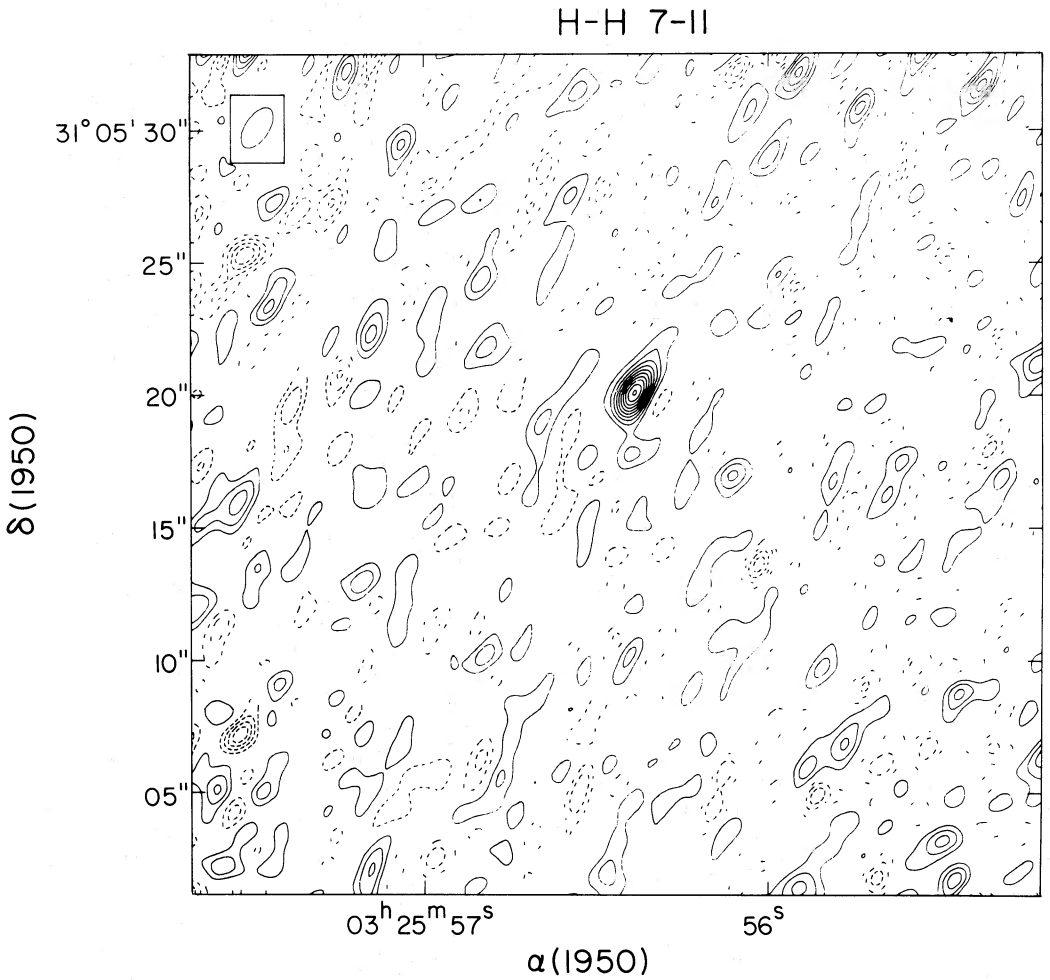

FIG. 9.—Aperture synthesis map of the H-H 7–11 region taken at 6 cm wavelength on the VLA. The map was cleaned and the restoration was made using the clean beam in the upper left hand corner of the map.

anomalously strong 1720 MHz emission is seen in a number of examples. The consistency of the velocity of emission among the three frequencies, the simplicity of the spectra and the low antenna temperatures suggest that this emission is not due to a maser process. The OH velocity of 8 km s^{-1} is close to the velocity measured for other molecules in this region (Lada *et al.* 1974). Sancisi *et al.* (1974) have mapped the OH emission over the entire Perseus OB2 dust cloud at 1667 MHz with the telescope of the Onsala Space Observatory. They find a peak in the thermal emission near H-H 7–11. From the ratio of the antenna temperature measured at Onsala to that at NRAO we estimate the angular size of the cloud to be about 20′. We conclude that any OH maser emission is weaker than 0.2 Jy at this time. At the same epoch a weak H_2O maser feature was present from source A with a velocity of -12 km s^{-1}.

III. DISCUSSION

a) Maser Source Properties

During our monitoring observations we have identified three spatially distinct H_2O masers in the vicinity of the Herbig-Haro objects 7–11. These sources display slightly different characteristics as evidenced by their positional relation to the H-H objects, their intensity, their velocity and the time variability of the latter two quantities.

The H_2O maser source A, the first one identified, has the curious property of being aligned with the H-H objects 7–11. The separation between the maser and H-H 11 is about equal to the separations among the H-H objects, $\sim 10^{17}$ cm or 20″ (see Fig. 1). The position of this maser lies just outside the error bars of the position of one of the 2.2 μm infrared sources. No continuum radiation at a wavelength of 6 cm was detected at the position of source A stronger than 0.5 mJy. Under the assumption of small optical depth at 5 GHz we conclude that if a star is present at the H_2O position, it must have a spectral type later than B3.6 (ZAMS) with the usual assumptions given in § II*c*. The velocity of the H_2O maser features has varied significantly on the time scale of months to years over a velocity range of ~ 30 km s^{-1}, but has maintained a substantial blueshift of between 15 and 40 km s^{-1} with respect to the ambient molecular

© American Astronomical Society • Provided by the NASA Astrophysics Data System

1980ApJ...237...26H

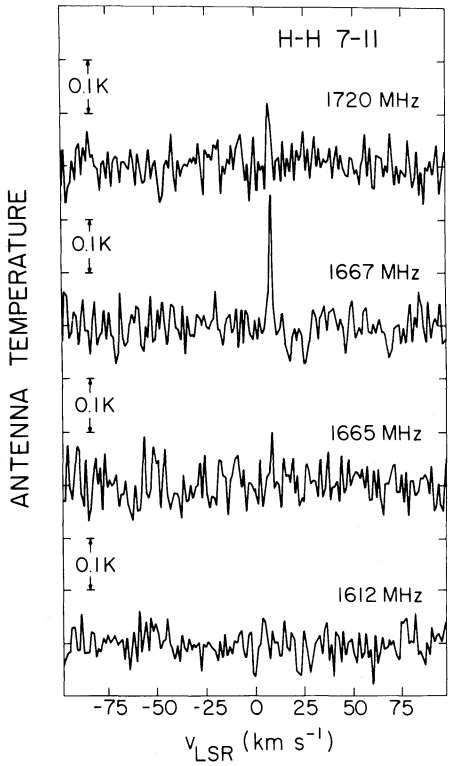

FIG. 10.—Spectra of H-H 7–11 taken on the NRAO 140 foot (43 m) telescope. The velocity axis refers to the local standard of rest and is based on the rest frequencies of 1720.533, 1667.379, 1665.402, and 1612.231 MHz for the four spectra given. The velocity resolution is 1.4 km s^{-1}.

cloud velocity of 8 km s^{-1}. Blueshifted emission is also observed in the nearby H-H objects, ranging from $\sim$30 km s^{-1} for H-H 10 to $\sim$147 km s^{-1} for H-H 11.

Source B is displaced from the axis of alignment of the H-H objects as well as from source A by 38″ or 3×10^{17} cm. A compact (<0″.4) H II region is coincident with source B to within the error limits of our measurements. The parameters for the H II region indicate the presence of a B3 (ZAMS) star which may be the exciting source for the maser radiation. There is no IR source at the maser position with a K magnitude less than 10. Both maser sources A and B have the same peak intensity of $\sim$200 Jy. The velocity of source B has varied over the relatively narrow range of 5 km s^{-1}, from 3 km s^{-1} up to about the cloud velocity of 8 km s^{-1}, compared to the 30 km s^{-1} range of velocities observed in source A. Both source A and source B have displayed rapid amplitude variations in their spectra on a time scale of less than a week.

Source C also displays velocity features close to the ambient cloud velocity which, at its position, is 7.6 km s^{-1}. In like manner to source B, the features display a slight blueshift in their velocity which have varied from 2.3 to 7.3 km s^{-1}. This source is considerably weaker than either source A or B, its peak flux density has not exceeded $\sim$10 Jy since it was initially observed in 1976 December. Source C is displaced from the other H_2O masers and H-H objects by $\sim 1 \times 10^{18}$ cm. However, all three masers lie within equal brightness contour levels of the NH_3 emission from this region (see Fig. 1).

b) Time Variations

The integrated flux densities of the three masers are plotted versus time in Figure 11. The time variations of the H_2O maser sources A and B are characterized by periods of activity, when the flux of the maser is >5 Jy, lasting for $\sim$12 months, followed by periods of $\sim$2–18 months, in which any maser emission is below our sensitivity limits. During the active phase, individual maser features appear and disappear at random velocities on the time scale of a week to months. There was a tendency for the maser emission from source A to occur at velocities near ~ -11 km s^{-1} during the active period from 1977 September to 1978 April. During the active period reported by Lo *et al.* (1976) from 1974 May until 1976 February there was a similar tendency for the main center of activity to cluster around a velocity of -19 km s^{-1}. The spectra of the three maser sources have remained relatively simple in appearance, consisting of from one to three features at most times. As noted by Lo *et al.* (1976), different velocity features did not vary in unison, so a common radiative pump mechanism for the maser emission is improbable. It is curious, however, that after an 18 month period of quiescence, both sources A and B turned on within 10 days of each other in 1977 September (see Fig. 3). The B source subsequently disappeared while the A source remained at a level of $\sim$40 Jy. Such an occurrence seems unlikely unless the two masers are located equidistant from a common pump source. Further observations are required to substantiate this idea.

The integrated flux of the A source is seen to increase to a maximum slowly but erratically over 2 to 6 months having peaks in the intensity every 1 to 2 months. If we assume that these time variations are due to motion of an exciting source capable of producing maser emission on encountering the clumpy interstellar medium, we deduce a separation for the cloudlets as well as a separation of regions of enhanced density. For example, the periods of quiescence of $\sim$1 year would correspond to movement of the source through a region of low density matter. Assuming a velocity of $\sim$20 km s^{-1} we obtain a separation of 6×10^{13} cm. The separation between individual cloudlets would be of the order of 5×10^{12} cm.

IV. SOURCE MODELS

One may expect a complete model for the H-H 7–11 region to explain the apparent physical association of the H_2O masers with the H-H objects, the IR sources, and molecular cloud as well as the unusual properties of the H-H objects and the H_2O masers. Böhm (1978) reviews a number of proposals which have been made to explain some of the properties of the H-H objects. Strom, Grasdalen, and Strom (1974) suggested that the H-H objects are reflection nebulae illuminated by optically invisible stars indicated by

© American Astronomical Society • Provided by the NASA Astrophysics Data System

1980ApJ...237...26H

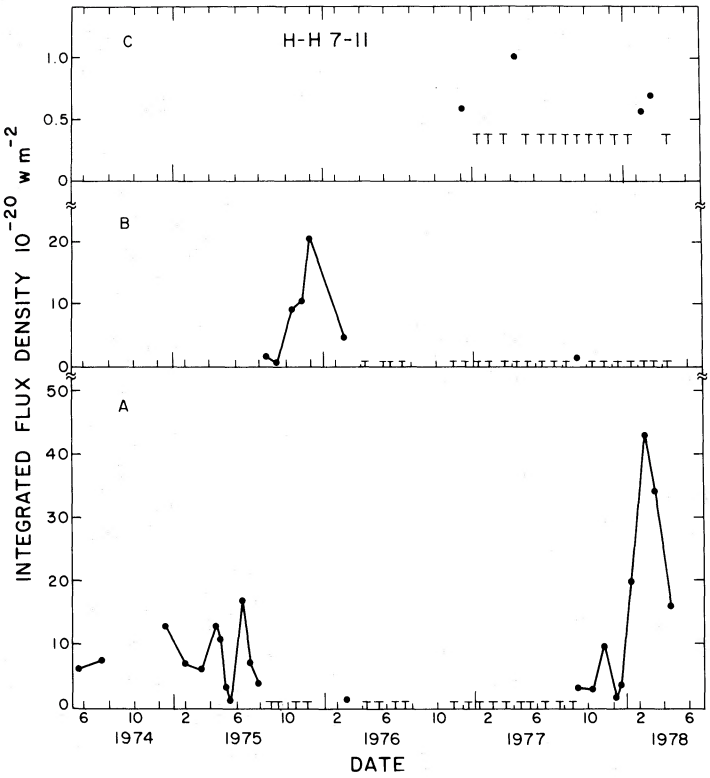

FIG 11.—Integrated flux density versus time for the three maser sources. The upper limits for detection for sources A and B are 0.4×10^{20} W m^{-2}.

IR sources. This suggestion has met with a number of difficulties (see Schwartz 1975, 1978; Dopita 1978*a*). The main problem is that differences are observed in the emission spectra of some H-H objects in regions separated by only a few seconds of arc, yet which persist for periods of time longer than the light travel time. This would rule out the model of a single illuminating source in these H-H objects.

A number of shock wave models have been advanced for H-H objects following from the initial hypothesis by Schwartz (1975) that T Tauri nebulae, which have similar spectra to H-H objects, result from radiatively cooling gas behind a shock front. Münch (1977), Dopita (1978*a*, *b*), and Raymond (1979) have found that the optical emission towards several H-H objects is consistent with that expected from shock excited material. The energy sources responsible for the shock waves are obscured stellar or protostellar objects.

Dopita (1978*b*) has suggested two types of stellar objects as energy sources. The first is a star undergoing an FU Orionis type event. The second is a B-type star in which the H-H objects may be identified with fragments of a "cocoon" which has been broken up and driven outward by radiation pressure. Schwartz (1978) has proposed a model in which a strong stellar wind from an embedded pre–main-sequence star produces shock waves upon interaction with small ambient cloudlets. The H-H objects become visible as the shocked stellar wind material cools. A similar model has been suggested by Canto (1978). Rodriguez *et al.* (1979) argue that the model fails to explain the high velocities commonly found in H-H objects because the post shock velocities of the wind are too low. Both the shocked cloudlet model (Dopita 1978*b*) and the shocked stellar wind model (Schwartz 1978; Canto 1978) require the exciting source to be relatively close to (within 0.1 pc) the H-H objects. This is entirely consistent with our results for the H-H 7–11 region where the possible centers of excitation, namely the IR, the H_2O maser, and the radio continuum sources, all lie in the range of 0.03–0.3 pc from the H-H objects. However, in a radio survey of a larger sample of H-H objects, Rodriguez *et al.* (1979) found compact H II regions, which are indicative of early B-type stars, within 0.2 pc of the H_2O masers, but separated from the H-H objects by an average distance of ~ 1 pc. From these results Rodriguez *et al.* (1979) suggest a model in which the H-H objects are discrete high velocity ejections from early B-type stars. The high velocity H_2O masers represent an earlier phase of evolution of the ejecta, thus their proximity to the H II regions. On the basis of theoretical considerations Norman and Silk (1979) have proposed a similar association between H_2O masers and the H-H phenomenon. In their model Rayleigh-Taylor instabilities in the shell, which are produced from the interaction of a supersonic wind from a young pre–T Tauri star with the surrounding molecular cloud, lead to infalling clumps of material confined by ram pressure. These clumps are eventually blown outward and accelerated to high velocities of ~ 100 km s^{-1} by

© American Astronomical Society • Provided by the NASA Astrophysics Data System

1980ApJ...237...26H

the stellar wind. As the fragments or "interstellar bullets" are decelerated again upon interaction with the ambient medium, they radiate as H-H objects. The low and high velocity H_2O masers occur in this model during the infall and acceleration phase of the clumps.

The morphology and kinematics of the H-H 7–11 region can be partially described in terms of the interstellar bullet theory. If we consider the compact H II region as the site of the protostar that produces the interstellar bullets, the coincident H_2O source B would represent the low velocity H_2O phase of the ejecta and the A source lying at a projected distance of 0.1 pc, would represent the high velocity phase. The H-H objects 7–11 are situated at greater distances of 0.1 to 0.3 pc from the protostar, in accordance with the theory. However, the H_2O source C would need a separate energy source because of its large separation from the H II region (0.4 pc) and its low velocity with respect to the molecular cloud.

The interstellar bullet theory has a number of difficulties. The most notable difficulty is the lack of a suitable energy source capable of accounting for the ejection. Calculations by Strel'nitskii and Sunyaev (1973) require a stellar wind from a luminous O-type star to accelerate the condensations to the observed high velocities of ~ 100 km s^{-1}. Such stars have not been found in the vicinity of H-H objects. Furthermore, the time scales for Rayleigh-Taylor and Kelvin-Helmholtz instabilities may be too short to allow the high velocity condensations to develop into H-H objects.

The large number of different velocity components and the range of velocities of the H_2O maser source A in the H-H 7–11 region also present a problem for the interstellar bullet theory. This would require a large number of bullets (~ 30) to have been ejected in a highly collimated beam with respect to the exciting source (B) and to have passed through the maser phase at the same distance from the ejecting source independent of velocity. The VLBI observations show that at least three velocity components spread over 10 km s^{-1} in velocity lie within a projected region having a diameter smaller than 7×10^{13} cm. Had these bullets travelled a distance of 10^{17} cm at a mean velocity of ~ 20 km s^{-1} we would expect the spatial separation to be much larger than 7×10^{13} cm. If the theory were correct, the particular clouds which became masers would appear to be breaking up as they mase and could not be destined to become H-H objects.

Because of the problems described above and because the interstellar bullet description of the H-H 7–11 region at best involves a combination of individual stars and high velocity ejecta, we favor the view that a number of stars of different types are forming in the same general region. There are too many distinct compact objects in the region to be explained in terms of a single energy source. The IR objects, the compact H II region, the H_2O masers, and the H-H objects are probably manifestations of stars of different masses in different evolutionary stages. The presence of other young stellar objects such as Hα-emission objects and T Tauri stars adds support to the conclusion that stars of various types are forming in this region. The connection between H-H objects and compact sources of IR, H II, and maser emission is not clear. The H_2O masers and Herbig-Haro objects may be high velocity cloud fragments, but they may not be ejected or accelerated by the same stars. Lo *et al.* (1976) suggest a model in which the stellar wind from a pre–main-sequence star creates a cavity in the molecular cloud around the star. The H_2O masers arise in the transition region between the stellar wind zone and the undisturbed molecular cloud. This model is entirely consistent with our observations. There are several possible explanations for the prevalence of blueshifted emission from the H-H objects and H_2O masers. H-H objects may be expanding away from the exciting source in all directions. However, the redshifted components, i.e., those moving away from the observer, are burying themselves deeper in the molecular cloud where they become invisible due to extinction, whereas the blueshifted ones are moving closer to the surface of the cloud where the optical extinction is lower. Similarly, redshifted maser emission from an expanding stellar envelope may be blocked from the observer's view by the optically thick H II region. Only the blueshifted maser emission may be visible for a variety of other reasons. For example, if amplification of the continuum radiation from an H II region around an exciting star is important, only those components expanding towards the observer would be seen. In this case the extent over which H_2O maser features are found in a particular source would place a lower limit on the size of the H II region. The VLBI results for source A indicate a limit of 7×10^{13} cm. The lack of IR sources near masers B and C can be explained by assuming that they are buried deep in the molecular cloud where the extinction is much greater than it is towards maser source A.

The tendency for the H_2O masers, the H-H objects, and, to a certain extent, the IR sources, to lie along the edge of the molecular cloud as indicated by the NH_3 brightness contours also occurs in some of the H II regions which Ho (1977) has mapped in NH_3 (e.g., S140, S255, and S235) where the H_2O emission occurs on the edge of the neutral cloud. The formation of more massive OB stars is observed to occur along the interface of expanding H II regions and a dense molecular cloud (see Elmegreen and Lada 1977). Ionization-shock fronts are deemed responsible for this OB star formation, but lower mass stars are suggested as arising from the collapse of undisturbed cloud fragments and may occur anywhere within the dark cloud. The results for H-H 7–11 imply that low mass stars also seem to form preferentially along the edge of molecular clouds. Loren (1976) has suggested that the collision between two molecular clouds has initiated the star formation, but Ho and Barrett (1979) find no evidence from their NH_3 observations for such a collision. They suggest a picture in which cloud fragments collapse with minimal interaction with the ambient cloud. The cloud fragments disappear and are replaced by stars. This explains why the possible signposts of star formation do not occur at peak

© American Astronomical Society • Provided by the NASA Astrophysics Data System

1980ApJ...237...26H

density of the molecular cloud. The presently observed cloud fragment represents the site of future star production.

V. SUMMARY

The molecular cloud containing the H-H objects 7–11 is an interesting region of star formation. We have identified three sites of H_2O maser emission and monitored them over a period of 3 years. These masers are unusually small in dimension and vary more rapidly than most other masers. We have also discovered a compact H II region, close to one of the masers which corresponds to a B3 star. The recently proposed interstellar bullet theory of H-H objects, in which the H-H objects are evolved H_2O maser fragments, is attractive because it connects the maser and H-H phenomena. However, it does not satisfactorily explain all the morphological features of the H-H objects and masers. We prefer a simple model in which a cluster of stars of different type have formed in the same vicinity. The H-H objects have their own excitation mechanism independent of the ones for the H_2O masers and compact H II region.

We acknowledge stimulating discussions with P. T. P. Ho, who allowed us to use his NH_3 data prior to publication, and G. H. Herbig. We would like to thank the Haystack staff for their help. We thank B. Ronnang and the staff at Onsala Space Observatory; R. Genzel, Dennis Downes, and the staff at the Max Planck Institute for Radio Astronomy; L. I. Matveyenko, V. Kostenko, L. Kogan, I. I. Moiseev, and the staff of the Crimean Astrophysical Observatory for their assistance with the VLBI experiment. The work of J. A. G. B. was supported in part by the Consejo Nacional de Ciencia y Tecnologia, Mexico. Work at the M.I.T. Research Laboratory of Electronics is supported in part by a grant from the National Science Foundation.

REFERENCES

Böhm, K. H. 1978, in *Protostars and Planets*, ed. T. Gehrels (Tucson: University of Arizona Press), p. 632.
Balonek, T. 1979, private communication.
Canto, J. 1978, *Astr. Ap.*, **70**, 11.
Dickinson, D. F., Kojoian, G., and Strom, S. E. 1974, *Ap. J. (Letters)*, **194**, L93.
Dopita, M. A. 1978*a*, *Ap. J. Suppl.*, **37**, 117.
———. 1978*b*, *Astr. Ap.*, **63**, 237.
Duffett-Smith, P. J., and Readhead, A. C. S. 1976, *M.N.R.A.S.*, **174**, 7.
Elmegreen, B. G., and Lada, C. J. 1977, *Ap. J.*, **214**, 725.
Genzel, R., *et al.* 1979, *Astr. Ap.*, **78**, 239.
Herbig, G. H. 1974, *Lick Obs. Bull.*, **658**, p. 1.
Herbig, G. H., and Rao, N. K. 1972, *Ap. J.*, **174**, 401.
Ho, P. T. P. 1977, Ph.D. thesis, Massachusetts Institute of Technology.
Ho, P. T. P., and Barrett, A. H. 1979, in preparation.
Högbom, J. A. 1974, *Astr. Ap. Suppl.*, **15**, 417.
Lada, C. J., Gottlieb, C. A., Litvak, M. M., and Lilley, A. E. 1974, *Ap. J.*, **194**, 609.
Lo, K. Y., Burke, B. F., and Haschick, A. D. 1975, *Ap. J.*, **202**, 81.
Lo, K. Y., Morris, M., Moran, J. M., and Haschick, A. D. 1976, *Ap. J. (Letters)*, **204**, L21.
Loren, R. B. 1976, *Ap. J.*, **209**, 466.
Münch, G. 1977, *Ap. J. (Letters)*, **212**, L77.
Norman, C. A., and Silk, J. 1979, *Ap. J.*, **228**, 197.
Panagia, N. 1973, *Astr. Ap.*, **78**, 929.
Panagia, N., and Felli, M. 1975, *Astr. Ap.*, **39**, 1.
Raymond, J. C. 1979, *Ap. J. Suppl.*, **39**, 1.
Rodriguez, L. F., Moran, J. M., Ho, P. T. P., and Gottlieb, E. W. 1980, *Ap. J.*, **235**, 845.
Sancisi, R., Goss, W. M., Anderson, C., Johnsson, L. E. B., and Winnberg, A. 1974, *Astr. Ap.*, **35**, 445.
Schraml, J., and Mezger, P. G. 1969, *Ap. J.*, **156**, 269.
Schwartz, R. D. 1975, *Ap. J.*, **195**, 631.
———. 1978, *Ap. J.*, **223**, 884.
Strel'nitskii, V. S., and Sunyaev, R. A. 1973, *Soviet Astr.—AJ*, **16**, 579.
Strom, S. E., Grasdalen, G. L., and Strom, K. M. 1974, *Ap. J.*, **191**, 111.
Strom, S. E., Vrba, F. J., and Strom, K. M. 1976, *A.J.*, **81**, 314.
Turner, B. E. 1973, *Ap. J.*, **186**, 357.
White, G. J., and Little, L. T. 1975, *Ap. Letters*, **16**, 151.

B. F. Burke, P. Greenfield, and J. A. Garcia-Barreto: 26-335, Research Laboratory of Electronics, Massachusetts Institute of Technology, Cambridge, MA 02139

A. D. Haschick and J. M. Moran: Center for Astrophysics, 60 Garden Street, Cambridge, MA 02138

L. F. Rodriguez: Instituto de Astronomia, Universidad de Mexico, APDO Postal 70-264, Mexico, 20, DF, Mexico

© American Astronomical Society • Provided by the NASA Astrophysics Data System